Universiteit Leiden
The Netherlands

Diseases of the nervous system associated with calcium channelopathies

Todorov, B.B.

Citation

Todorov, B. B. (2010, June 2). *Diseases of the nervous system associated with calcium channelopathies*. Retrieved from https://hdl.handle.net/1887/15580

Version:	Corrected Publisher's Version
License:	Licence agreement concerning inclusion of doctoral thesis in the Institutional Repository of the University of Leiden
Downloaded from:	https://hdl.handle.net/1887/15580

Note: To cite this publication please use the final published version (if applicable).

GENERATION AND CHARACTERIZATION OF TRANSGENIC MICE EXPRESSING T666M MUTANT $CA_v2.1\ \alpha_1$ SUBUNITS IN PURKINJE CELLS

Boyan Todorov,[1] Simone Houtman,[3] Freek Hoebeek,[3]
Ludo A.M. Broos,[1] Yongjun Qin,[1,2] Rune R. Frants,[1]
Chris I. de Zeeuw,[3,4] Arn M.J.M. van den Maagdenberg[1,2]

Departments of [1]Human Genetics and [2]Neurology, Leiden University Medical Center, Leiden, The Netherlands; [3]Department of Neuroscience, Erasmus MC Rotterdam, Rotterdam, The Netherlands; [4]Netherlands Institute for Neuroscience, Royal Dutch Academy for Sciences, Amsterdam, The Netherlands;

Manuscript in preparation

ABSTRACT

Voltage-gated $Ca_V2.1$ calcium channels are important for neurotransmitter release in most brain synapses. The channel's pore-forming α_{1A} subunit is encoded by the *CACNA1A* gene and is mutated in patients with Familial Hemiplegic Migraine type 1 (FHM1). Most FHM1 patients who carry the missense T666M mutation suffer from permanent cerebellar ataxia, in addition to their hemiplegic migraine. At the single channel level, the T666M mutation causes an increased neuronal Ca^{2+} influx (i.e., a gain-of-function effect). Both knockout and knockin (i.e., with the FHM1 S218L mutation) *Cacna1a* mice, carrying respectively a loss and a gain of function of $Ca_V2.1$ mutations, were shown to have cerebellar ataxia. As $Ca_V2.1$ channels are expressed throughout the brain, these mice are not suited to determine which cell types contribute most to the ataxic phenotype. Recently generated, Purkinje cell-specific knockout mice clearly showed that ablation of $Ca_V2.1$ channels in Purkinje cells alone is sufficient to cause ataxia. However, it is not known whether Purkinje cell-specific expression of a gain-of-function mutation has the same outcome. Therefore, we generated transgenic mice overexpressing human *CACNA1A* cDNA containing the FHM1 T666M mutation exclusively in Purkinje cells. The transgene was designed in such a way that EGFP was expressed from the same bicistronic messenger, allowing the indirect analysis of mutant α_{1A} protein in the presence of endogenous α_{1A} protein. Three transgenic mouse lines were obtained that differed in transgene copy number and expression level. None of them showed signs of abnormal motor behavior, which may be due to the relatively low expression levels of the transgene. It was not investigated whether the T666M-mutated $Ca_V2.1$ channels cause subtle effects on Purkinje cell functioning.

Keywords: Purkinje neurons, $Ca_V2.1$, P/Q-type Ca^{2+} channels, *CACNA1A*, cerebellar ataxia

Abbreviations:
ACh – acetylcholine
CNS – central nervous system
KO – knockout
EGFP – enhanced green fluorescent protein
IRES – internal ribosome entry site
PC – Purkinje cell
L7(pcp-2) – L7 Purkinje cell-specific protein

INTRODUCTION

Neuronal $Ca_V2.1$ (P/Q-type) voltage-gated Ca^{2+} channels (VGCC) are present at most synapses of the central nervous system (*Westenbroek et al., 1995*). One major function of these channels is to regulate presynaptic Ca^{2+} entry and neurotransmitter release. Although several Ca_V subtypes can be involved in this process, in certain neurons such as Purkinje cells, over 90% of VGCC-dependent Ca^{2+} entry relies on $Ca_V2.1$ channels alone (*Mintz et al., 1992*). The pore-forming α_{1A} subunit of $Ca_V2.1$ channels that is encoded by the *CACNA1A* gene is mutated in several neurological disorders, such as Familial Hemiplegic Migraine type 1 (FHM1) and Episodic Ataxia type 2 (EA2) (*Ophoff et al., 1996*). The most common mutation in FHM1 is a threonine to methionine substitution at position 666 (T666M) (*Ophoff et al., 1996; Ducros et al., 1999*). Most FHM1 patients carrying the mutation also suffer from permanent cerebellar ataxia (*Kors et al., 2003*). Electrophysiological analyses revealed that T666M-mutated $Ca_V2.1$ channels have a 60% reduction in P/Q-type current density (*Hans et al., 1999*). Subsequent single channel recordings in transfected cerebellar granule cell neurons of $Ca_V2.1$-deficient mice (*Fletcher et al., 2001*) revealed that the T666M mutation causes a negative shift in channel activation, resulting in an increased Ca^{2+} influx (i.e., a *gain-of-function*); this increase was particularly evident at low voltages (*Tottene et al., 2002*). However, the exact electrophysiological properties of the T666M mutation are debated, as a left-shift in voltage activation could not be confirmed by others (*Cao et al., 2004),* and may be due to the use of other accessory $Ca_V2.1$ subunits and *CACNA1A* splice forms.

The relation between $Ca_V2.1$ α_1 mutations and the presence of cerebellar ataxia is intriguing, since both gain- and loss-of-function mutations are associated with loss of gait (*van den Maagdenberg et al., 2007*). Studies in natural mouse mutants with loss-of-function *Cacna1a* mutations have suggested that cerebellar ataxia results from increased irregularity (so-called noise) in the firing of Purkinje cell neurons (*Hoebeek et al., 2005; Walter et al., 2006*). The FHM1 S218L mutation, which has a gain-of-function effect on Ca^{2+} influx (*Tottene et al., 2002*), was also shown to increase the noise in Purkinje cell firing (*data unpublished*) in knockin mice (*van den Maagdenberg et al., 2010*). However, cell type-specific contributions to the ataxic phenotype could not be assessed in these mouse models, due to the widespread expression of the mutant $Ca_V2.1$ channels in the cerebellum and the rest of the brain.

Several genetic ataxic mouse models have indicated that Purkinje cells play a pivotal role in cerebellar ataxia (*for review, see Fletcher & Frankel, 1999*). Moreover, unpublished data from Purkinje cell-specific $Ca_V2.1$ knockout mice showed that the same is true for $Ca_V2.1$-related cerebellar ataxia. Therefore, we set out to generate transgenic mice overexpressing the mutant human $Ca_V2.1$ α_1 protein in Purkinje cells. Transgene expression in these mice is driven by the Purkinje cell-specific *L7/Pcp-2* promotor (*Barski et al., 2000*). The most predominant Purkinje cell type-specific splice form (PC-type) of *CACNA1A* (*Soong et al., 2002*) was selected as the cDNA backbone. The cDNA

was mutated to encode for the FHM1 T666M substitution in the human α_{1A} protein. To allow for (indirect) detection of human mutated α_{1A} protein in mice that also express endogenous α_{1A} protein, enhanced green fluorescent protein (EGFP) reporter and the mutant protein were expressed from the same messenger, using an internal ribosome entry site (IRES) (*for review, see Balvay et al., 2009*) in the construct.

Three transgenic mouse lines were obtained that differed in transgene copy number and the expression level of the transgene. No ataxic phenotype was observed. The relatively low expression level of the transgene, however, might have obscured other possible consequences of the T666M mutation in these transgenic mice.

EXPERIMENTAL PROCEDURES

Generation of constructs

The IRES sequence of the encephalomyocarditis virus (EMCV) was fused to the coding sequence of EGFP to create a reporter cassette that was inserted into the *Bam*HI site of exon 4 of the (modified) *Pcp2* (*L7*) (*Fig. 1A*) gene (in expression vector L7ΔAUG (*Smeyne et al., 1995*)). To assess the functionality of the IRES, a control construct was made by inserting the coding sequence of *Discosoma sp.* red fluorescent protein (dsRED) into the same *Bam*HI site, thus in front of the IRES. The insert that contained the dsRED- and EGFP-containing reporter cassette was excised with *Asu*II and *Cla*I and cloned into the pSG8 expression vector driven by the CMV promoter (*Cuppen et al., 1998*) to generate the construct CMV/dsRED-IRES-EGFP (*Fig. 1*).

For the transgene construct, human *CACNA1A* cDNA was used that corresponds to the most predominant Purkinje cell-specific splice form (*Jurkat-Rott & Lehmann-Horn, 2004; Kanumilli et al., 2006*). This cDNA lacks alternatively spliced exon 31a (-NP) (*Bourinet et al., 1999*) and contains the alternatively spliced longer form of exon 47. The FHM1 mutation T666M was introduced into the *CACNA1A* cDNA by

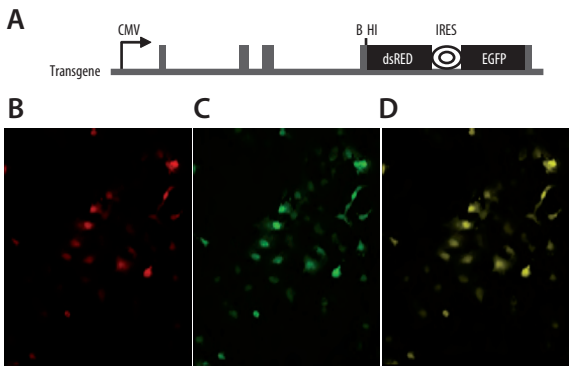

Figure 1. Analysis of bicistronic reporter construct in COS-1 cells. (A) Schematic representation of the CMV/dsRED-IRES-EGFP construct with the position of the CMV promoter, the IRES, and dsRED and EGFP cDNAs. Grey boxes correspond to exons of the L7 gene; black boxes to translated regions; the striped box to the IRES **(B-D)** Fluorescence microscopy reveals expression of red-fluorescent dsRED protein (B), green-fluorescent EGFP protein (C), and perfect co-localization of green and red signals in merged pictures (D).

mutagenesis. In the final construct, the *CACNA1A* cDNA was cloned into the reporter cassette to generate construct L7/CACNA1A^{T666M}-IRES-EGFP (see *Fig. 2*).

Cell culture and transfection

COS-1 cells were maintained in DMEM without phenol red (*Invitrogen, Carlsbad, CA*), supplemented with 10% fetal bovine serum (FBS), L-glutamine (2 nM), and glucose (100 ×) (all from *Invitrogen*). Cells were cultured in an incubator with 5% CO_2 at 37°C. Twenty-four hours prior to transfection, 1×10^5 COS-1 cells were seeded onto 24-well (35-mm) culture dishes with coverslips (20 × 20 mm). Cells in each well were transfected with 1 μg CMV/dsRED-IRES-EGFP using Fugene (*Boehringer Mannheim, Mannheim, Germany*), according to the manufacturer's instructions. After 48 h, cells were fixed and analyzed by fluorescence microscopy.

Generation of transgenic mice

The transgene construct was excised from the expression vector L7/CACNA1A^{T666M}-IRES-EGFP using *Asu*II and *Cla*I (*Fig. 2*). The transgene construct was purified and microinjected into the male pronucleus of fertilized eggs of *C57Bl6/Ico* mice. Transgenic offspring were identified by Southern blotting of *Eco*RV and *Xho*I-digested tail DNA and hybridization with a L7-specific probe (*Fig. 2B, C*). The number of transgene copies integrated into the genome was estimated by comparing the intensities of the endogenous *L7* band and transgene-derived band on Southern blotting using ImageQuant TL software (*GE Healthcare, Bucks, UK*) for each line. Three independent transgenic lines were obtained. For genotyping, EGFP primers P1 (5`-cgataataccatggtgagcaagggcgag-3`) and P2 (5`-tccccgcgggctttacttgtacagctcgt-3`) were used in a PCR using genomic tail DNA as a template.

RNA analysis

Total RNA was isolated from freshly dissected cerebella and cerebra from 6-week-old mice according to standard procedures. For RT-PCR, first-strand cDNA was synthesized using random primers. For quantitative PCR analysis, mouse- and human-specific forward primers P3 (5`-ttctctctggaatgtgtgctg-3`) and P4 (5`-ttctctctcgaatgtgtgtgctc-3`), respectively, were used together with reverse primer P5 (5`- gctcaggttgatgaagttattcc-3`), which recognizes Purkinje cell-specific *Cacna1a*$^{-NP}$ cDNAs of both human and mice sequences. Amplification efficiencies of both PCRs were shown to be similar (*data not shown*). As an internal reference, the *β-actin* gene was amplified using primers P6 (5'-taaaacgcagctcagtaacagtccg-3') and P7 (5`-tggaatcctgtggcatccatgaaac-3`). Results of the quantitative PCR were represented as Ct values, where Ct was defined as the threshold cycle of PCR at which amplified product was detected. The ΔCt was the difference in the Ct values derived from the transcript of interest (i.e. the transgene or the endogenous *Cacna1a*$^{-NP}$), and the reference *b-actin* transcript in the sample. The relative expression of the transgene compared to that of the endogenous *Cacna1a*$^{-NP}$ in

this case is the quotient of the $2^{-\Delta Ct}$ values for the two genes. The relative reduction in the expression of the endogenous *Cacna1a*$^{-NP}$ in the samples of the mutant mice, was determined using the ΔΔCt method (*Yuan et al., 2007*), where ΔCt values for *Cacna1a*$^{-NP}$ in samples of wild-type mice were extracted from the ΔCt values for *Cacna1a*$^{-NP}$ in samples of the transgenics (ΔΔCt). The reduction in the expression of the *Cacna1a*$^{-NP}$ in transgenic mice, equals $1 - 2^{-\Delta\Delta Ct}$. Data are presented as means ± SD.

In situ hybridization

In situ hybridization was performed as described earlier (*French et al., 2001*). In brief, 40-µm thick sagittal sections were obtained from freshly dissected brains that were quickly thawed, fixed in 4% paraformaldehyde, acetylated in 1.4% triethanolamine and 0.25% acetic anhydride, dehydrated through graded ethanol solutions, and delipidated in chloroform. Next, the sections were hybridized overnight at 42°C in 100 µl buffer containing 50% formamide, 4×SSC, 10% dextran sulfate, 5×Denhardt's solution, 200 mg/ml cleaved salmon testis DNA, 100 mg/ml long-chain polyadenylic acid, 25 mM sodium phosphate (pH 7.0), 1 mM sodium pyrophosphate, and 100,000 CPM radiolabeled probe (~1 ng/ml) under parafilm coverslips. The sections were subsequently washed in 1×SSC at 55°C (30 min) and 0.1×SSC at room temperature (5 min), and dehydrated in ethanol. Hybridized sections were then exposed to autoradiographic film. ^{35}S-ATP end-labeled probes (*Amersham, Munich, Germany*) were generated using terminal deoxynucleotidyl transferase (*Promega, Leiden, The Netherlands*) according to the manufacturer's instructions. A 50-fold excess of unlabeled antisense oligonucleotide was used as negative control. The sequence of the antisense *L7* probe was 5`-agcactttacgtgttcatagggtcctctcctttcctgcctagaga–3`. Quantification of the signal strength was obtained using ImageJ software (*National Institutes of Health, Bethesda, MD*).

Immunohistochemistry

Brains from 6-week-old mice were obtained after cardiac perfusion with phosphate-buffered saline and 4% buffered paraformaldehyde; the brains were embedded in gelatine and cut in 40 µm-thick sagittal sections. Immunohistochemistry was performed using primary rabbit-anti-GFP antibody (AB290, 1:10,000; *Abcam, Cambridge, UK*) that was diluted in TBS containing 1% normal horse serum (NHS). The sections were incubated with primary antibody for 2hrs at room temperature and washed in TBS. Subsequently, the sections were incubated for 1h at room temperature with biotinylated goat-anti-rabbit antibody (1:200; *Vector Laboratories, Burlingame, CA)* that was diluted in the same buffer. After washing, the sections were incubated with avidin-biotin-peroxidase complex (ABC; *Vector Laboratories*) and stained with diaminobenzidine (DAB, 0.05%) as a chromogen. Finally, the sections were mounted on microscope slides.

Rotarod

Accelerating Rotarod (*UGO Basile S.R.L., Commerio VA, Italy*) tests were performed on a 4-cm diameter horizontal rotating rod. Tests were performed in a semi-dark room with a light source placed at the bottom to discourage the mice from jumping off the rod. Mice (10- 22 weeks old) were tested in groups of five. Following a training period (in which the mice were placed on the Rotarod turning at a low constant speed of 5 rpm for 5 min), the mice were subjected to 5 sessions (separated by a 30-min resting period) in a single day. Each trial started with the rod turning at a constant speed of 5 rpm for 10 s, after which the speed was gradually increased to 45 rpm over the following 5 min. The latency to fall (i.e., endurance) was recorded, and presented as mean ± standard error of the mean for each trial and genotype.

RESULTS

Here, we set out to generate transgenic mice overexpressing T666M-mutated $Ca_V2.1$ channels, exclusively in Purkinje cells. The most predominant *CACNA1A* cDNA of the human Purkinje cells was chosen and mutagenized to contain the T666M mutation.

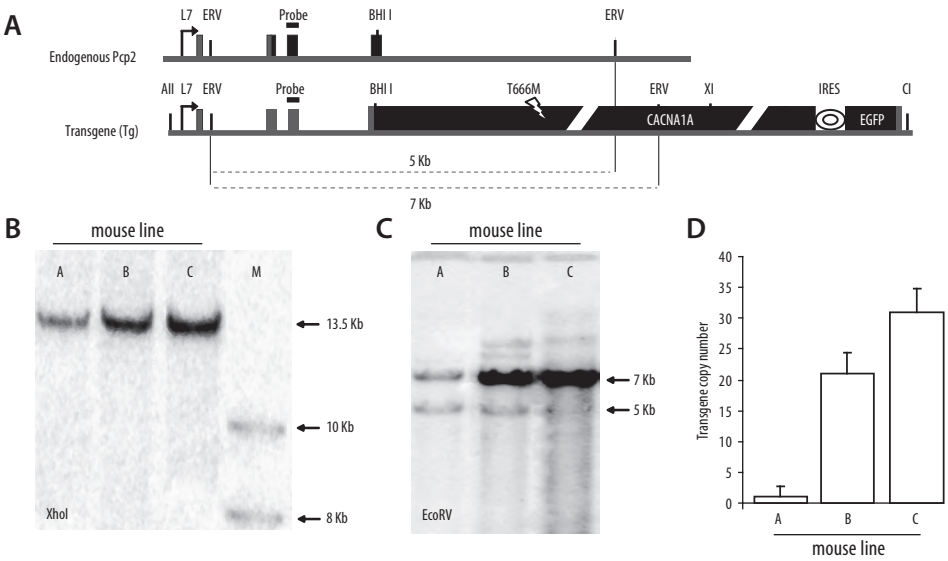

Figure 2. Generation of transgenic mice. (A) Schematic representation of the L7/CACNA1A^{T666M}-IRES-EGFP construct with the position of the L7 promotor, the IRES, and CACNA1A and EGFP cDNAs. Grey boxes correspond to exons of the L7 gene; black boxes to translated regions; the striped box to the IRES. The location of the probe for Southern analysis is indicated. Restriction sites: *A*II – *Asu*II; *E*RV – *Eco*RV; *X*I – *Xho*I; *B*HI – *Bam*HI; *C*I – *Cla*I. **(B)** Southern blotting of *Xho*I-digested genomic DNA hybridized with the internal L7 probe revealed that the genome of each line contained at least one complete transgene copy of 13.5 Kb. **(C)** Southern blotting of *Eco*RV-digested genomic DNA hybridized with the same probe showed an endogenous L7 band of 5 Kb and a transgene-derived band of 7 Kb. **(D)** Copy numbers of the transgene in the three transgenic lines. Pcp2 – Purkinje cell protein 2; endogenous *L7* gene; M – 1 Kb DNA ladder.

Purkinje cell-specific expression of the mutant protein was driven by the *L7* gene backbone of the construct, in which the *CACNA1A* cDNA was cloned. The *L7* gene was modified in the sense that all ATG codons in front of the translational start ATG of the cloned *CACNA1A* sequence were destroyed. Since no antibodies exist that can distinguish between mutant and endogenous α_{1A} protein, we designed the transgenic construct in such a way that both mutated α_{1A} protein and reporter EGFP were expressed from the same mRNA using an IRES. To assess the functionality of the IRES, we first studied a control construct which contained the cDNAs of fluorescent proteins dsRED and EGFP that were separated by an IRES sequence. Expression in this case was driven by the CMV promoter (*Fig. 1A*). Transfection of the construct in COS-1 cells showed comparable expression levels of dsRED (*Fig. 1B*) and EGFP (*Fig. 1C*) protein, as well as convincing co-expression (*Fig. 1D*) indicating that at the chosen position of the EGFP sequence relative to the IRES, the expression of the reporter gene is efficient and does not seem to interfere with the expression of the proximal gene.

For transgenesis, we generated a construct (i.e., L7/CACNA1A^{T666M}-IRES-EGFP) in which T666M-mutated *CACNA1A* cDNA was located in front of the IRES sequence (*Fig. 2A*). Three transgenic mouse lines were obtained. Southern blot analysis confirmed that at least one complete copy of the transgene (i.e., see ~13.5 Kb band in *Xho*I digests) had integrated into the genome of each of the three lines (*Fig. 2B*). By comparing the relative Southern blotting signals of transgene-derived (5 Kb) and endogenous (7 Kb) bands upon *EcoR*V digestion, it could be determined that lines A, B, and C contained 1, ~20, and ~30 copies of the transgene, respectively. Histological analyses did not reveal any gross abnormalities in cerebellar morphology or in Purkinje cell morphology or density in any of the lines (*data not shown*).

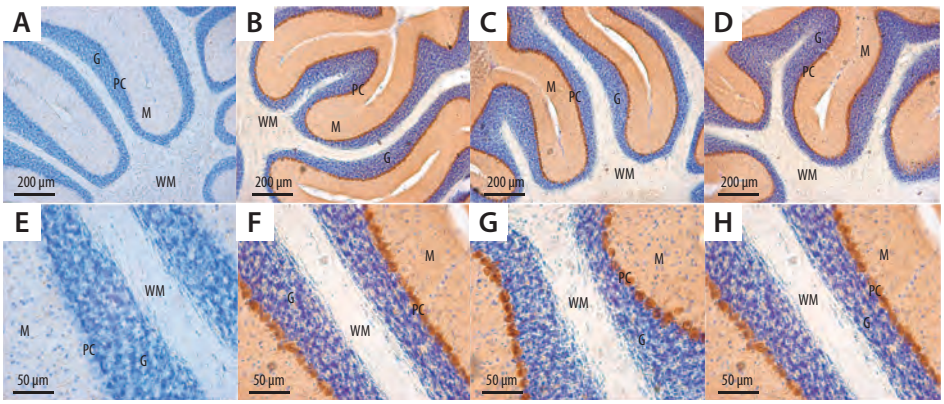

Figure 3. Green fluorescent protein immunostaining in the cerebellum of transgenic mice. Coronal cerebellar sections show the presence of EGFP (brown signal) in the Purkinje cell layer at lower **(A-D)** and higher **(E-F)** magnification. All sections were counter-stained with methylene blue. Panels a and e correspond to sections that were not stained with anti-GFP antibody. Wild type (A, E), line A (B, F), line B (C, G), and line C (D, H). G - granule cell layer; M - molecular cell layer; PC - Purkinje cell layer; WM - white matter.

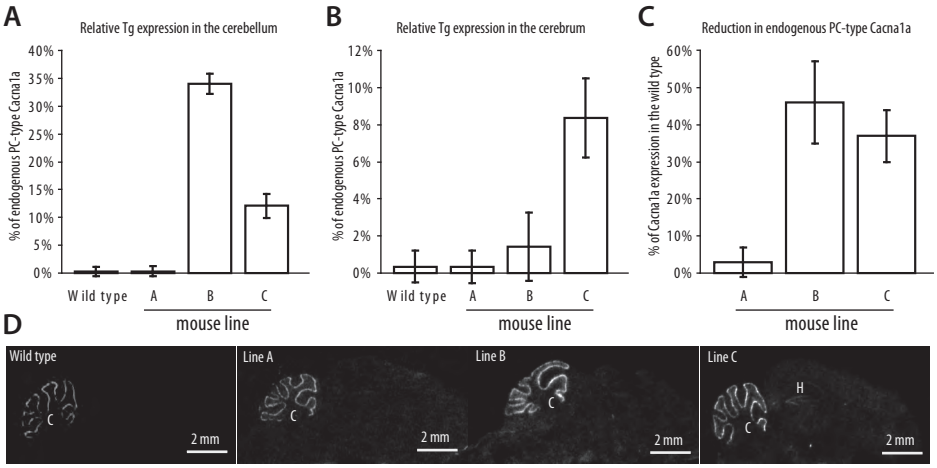

Figure 4. Endogenous and transgene-derived Cacna1a^{-NP} transcript levels in transgenic mice. (A) Transgene-derived *Cacna1a*$^{-NP}$ transgene expression level compared to endogenous *Cacna1a*$^{-NP}$ in cerebellar extracts of wild-type and transgenic mice. **(B)** Transgene-derived *Cacna1a*$^{-NP}$ transgene expression level compared to endogenous *Cacna1a*$^{-NP}$ in cerebral extracts of wild-type and transgenic mice. Only mice from line C show transgene expression outside of cerebellum. **(C)** Reduction of endogenous *Cacna1a*$^{-NP}$ in the cerebellum is only observed in lines B and C. **(D)** Radioactive *in situ* hybridization using labeled *L7*-antisense probe. No significant increase in signal strength was observed in the cerebellum of the transgenic mice compared to wild-type mice. Transgene expression is detectable in the hippocampal region in line C. C – cerebellum; H – hippocampus.

Cell-specificity of transgene expression was investigated by immunohistochemistry of reporter EGFP using anti-GFP antibody. A clear localization of the EGFP protein was noticed in Purkinje cells in all three lines (*Fig. 3B-D; enlarged in E-H*). Except for EGFP expression in the granule cells of the dentate gyrus in line C, no extracerebellar staining was observed (*data not shown*). These results show that the L7 promoter ensured Purkinje cell-specific expression of the transgene and that the bicystronic messenger is a target for the cell's translation machinery.

Real-time quantitative PCR (qPCR) was used to determine the relative expression levels of transgene-derived *CACNA1A* compared to the endogenous mouse *Cacna1a*$^{-NP}$ transcript in cerebellar extracts of mice from the three lines (*Fig. 4A*). *CACNA1A* expression in line B was ~34 ± 1.8% of that of the endogenous *Cacna1a*$^{-NP}$ level; in line C the relative expression of the transgene was even lower (~12 ± 2.1%), even though these mice carried larger numbers of transgene copies in their genome, compared to line B. For line A, the transgene gave hardly any expression (0.8 ± 0.3%). In line with the EGFP immunostaining results, some extra-cerebellar expression of the transgene was noticed by qPCR in mice from line C (i.e., 8.4 ± 1.8% of the endogenously expressed *Cacna1a*) (*Fig. 4B*). Interestingly, transgene expression seemed to downregulate the level of expression of endogenous *Cacna1a-*^{NP} transcripts in the cerebellum of lines B (48 ± 11%) and C (37 ± 7%) (*Fig. 4C*). Therefore, since the expression level of the transgene was determined relative

to the level of the *endogenous* gene, a downregulation of the latter gene means that the absolute level of the transgene as determined in *Figure 2* is in fact inflated.

Radioactive *in situ* hybridizations (ISH) were performed to further investigate cell-specific expression of the transgene in the cerebellum of the mutant mice. The *L7* antisense probe confirmed Purkinje cell-specificity of the L7 promoter (both in the endogenous L7 gene as in the construct), although a weak signal was obtained for the hippocampus of line C, in line with the EGFP immunostaining results. Since the intensity of the labeling in transgenic mice (carrying both transgene-derived as well as endogenous L7 transcripts) was not very different from that in non-transgenic wild-type mice, it could be concluded that the transgene expression in the mutants is very weak in comparison to the endogenous L7 expression (*Fig. 3D*).

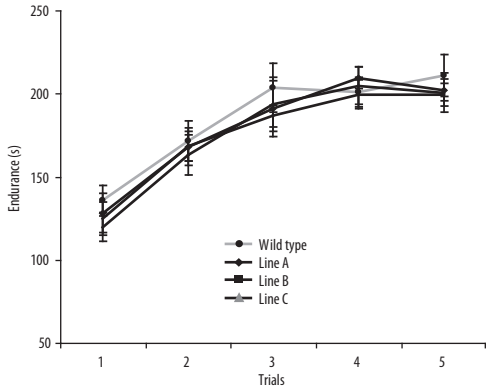

Figure 5. Motor behavior analysis using accelerating rotarod. No abnormalities in motor coordination nor motor learning were detected in the transgenic mice ($p > 0.8$). Endurance is plotted as the mean (± SEM) latency to fall of the rod for individual mice and trials.

Although *CACNA1A* expression in the transgene is rather low, we assessed whether the gain-of-function effect of the T666M mutation is large enough to result in a motor coordination phenotype. However, all transgenic mice performed well on accelerating rotarod (*Fig. 5*).

DISCUSSION

We used conventional transgenesis to generate mice that express T666M-mutant $Ca_V2.1$ channels selectively in Purkinje cells. As functional characteristics of multimeric $Ca_V2.1$ channels may differ depending on the isoforms of the individual subunits, attention was given to the *CACNA1A* cDNA that is present in the construct. Because alternative splicing, the underlying mechanism, is quite extensive in the *Cacna1a* gene (*Krovetz et al., 2000; Jurkat-Rott & Lehmann-Horn, 2004*), we decided to use the *CACNA1A* splice variant that is most abundantly expressed in Purkinje cells (*Soong et al., 2002*). Assessment of the expression of human T666M-mutated α_{1A} protein, on a background of endogenous mouse α_{1A} protein, was done by analyzing EGFP expressed from the same bicistronic messenger (using IRES sequence). We envisaged that co-expression of EGFP may also facilitate the *in vivo* tracing of axons of neurons expressing T666M-mutated α_{1A} protein (*Sekirnjak et al., 2003*). Transfection experiments in COS-1 cells

indicated that cloning a target sequence in front of the IRES sequence did result in comparable expression levels of the transgene and the reporter.

All three generated transgenic lines (A-C) expressed the transgene in the cerebellum. However, only in lines A and B was the transgene expression restricted to Purkinje cells as assessed by RNA *in situ* hybridization and EGFP protein immunohistochemistry. Line C showed additional ectopic expression in the dentate gyrus of the hippocampus. Our results indicate that the mRNA is expressed and is a suitable substrate for the cell's translational machinery. Because of the lack of species-specific α_{1A} antibodies, however, we have no means to assess whether the *CACNA1A* messenger is translated to α_{1A} protein. The clear EGFP expression suggests that the transgene is well expressed. However, the expression level of *CACNA1A*$^{-NP}$ was only ~34% (in line B) or ~12% (in line C) of the endogenous *Cacna1a*$^{-NP}$ level, and even lower when the fact that endogenous *Cacna1a*$^{-NP}$ expression is downregulated is taken into account. This indicates that at protein level α_{1A} expression is too low to reveal the functional consequences of T666M-mutated protein on Purkinje cell functioning. In line with this rationale, there were no indications that mutant $Ca_V2.1$ channels caused structural abnormalities to Purkinje cells or other neurons in the cerebellum.

Neither the reduction in the level of endogenous *Cacna1a*$^{-NP}$ transcripts nor the presence of T666M-mutant *Cacna1a*$^{-NP}$ transcripts in Purkinje cells resulted in motor coordination deficits in the transgenic mice, as was assessed by rotorod experiments. In retrospect, it could have been anticipated that the transgenic mice do not show signs of cerebellar ataxia. After all, heterozygous mice of either ataxic natural *Cacna1a* mutant mice or ataxic S218L knockin mice, carrying a *gain-in-function* $Ca_V2.1$ α_1 mutation, do not exhibit motor deficits (*Fletcher & Frankel, 1999; van den Maagdenberg et al., 2010*). Moreover, the left-shift in voltage activation of *T666M* mutant $Ca_V2.1$ channels was shown to be milder compared to that of, for instance, the S218L mutation (*Hans et al., 1999*). It remains a possibility, although rather unlikely, that the functional consequences of the T666M mutation may be mediated by another *CACNA1A* splice form and not by the one present in the transgene construct. Studying the firing behavior of mutant Purkinje cells will assess whether the T666M mutant $Ca_V2.1$ channels have a functional phenotype and address some of the questions discussed above.

ACKNOWLEDGEMENTS

This work was supported by grants from FP6 STREP EUROHEAD (to RR and AvdM), ZonMw (to CDZ and AvdM) and the Center for Medical Systems Biology (CMSB) established by the Netherlands Genomics Initiative/Netherlands Organisation for Scientific Research (NGI/NWO).

REFERENCES

1. Balvay L, Rifo RS, Ricci EP, Decimo D, Ohlmann T. Structural and functional diversity of viral IRESes. Biochim Biophys Acta. 2009 Jul 24 [Epub ahead of print].
2. Barski JJ, Dethleffsen K, Meyer M. Cre recombinase expression in cerebellar Purkinje cells. Genesis. 2000;28:93-8.
3. Bourinet E, Soong TW, Sutton K, Slaymaker S, Mathews E, Monteil A, Zamponi GW, Nargeot J, Snutch TP. Splicing of alpha 1A subunit gene generates phenotypic variants of P- and Q-type calcium channels. Nat Neurosci. 1999;2:407-15.
4. Cao YQ, Piedras-Rentería ES, Smith GB, Chen G, Harata NC, Tsien RW. Presynaptic Ca2+ channels compete for channel type-preferring slots in altered neurotransmission arising from Ca2+ channelopathy. Neuron. 2004;43:387-400.
5. Cuppen E, Gerrits H, Pepers B, Wieringa B, Hendriks W. PDZ motifs in PTP-BL and RIL bind to internal protein segments in the LIM domain protein RIL. Mol Biol Cell. 1998;9:671-83.
6. Ducros A, Denier C, Joutel A, Vahedi K, Michel A, Darcel F, Madigand M, Guerouaou D, Tison F, Julien J, Hirsch E, Chedru F, Bisgård C, Lucotte G, Després P, Billard C, Barthez MA, Ponsot G, Bousser MG, Tournier-Lasserve E. Recurrence of the T666M calcium channel CACNA1A gene mutation in familial hemiplegic migraine with progressive cerebellar ataxia. Am J Hum Genet. 1999;64:89-98.
7. Fletcher CF, Frankel WN. Ataxic mouse mutants and molecular mechanisms of absence epilepsy. Hum Mol Genet. 1999;8:1907-12.
8. Fletcher CF, Tottene A, Lennon VA, Wilson SM, Dubel SJ, Paylor R, Hosford DA, Tessarollo L, McEnery MW, Pietrobon D, Copeland NG, Jenkins NA. Dystonia and cerebellar atrophy in Cacna1a null mice lacking P/Q calcium channel activity. FASEB J. 2001;15:1288-90.
9. French PJ, O'Connor V, Voss K, Stean T, Hunt SP, Bliss TV. Seizure-induced gene expression in area CA1 of the mouse hippocampus. Eur J Neurosci. 2001;14:2037-41.
10. Hans M, Luvisetto S, Williams ME, Spagnolo M, Urrutia A, Tottene A, Brust PF, Johnson EC, Harpold MM, Stauderman KA, Pietrobon D. Functional consequences of mutations in the human alpha1A calcium channel subunit linked to familial hemiplegic migraine. J Neurosci. 1999;19:1610-9.
11. Hoebeek FE, Stahl JS, van Alphen AM, Schonewille M, Luo C, Rutteman M, van den Maagdenberg AM, Molenaar PC, Goossens HH, Frens MA, De Zeeuw CI. Increased noise level of purkinje cell activities minimizes impact of their modulation during sensorimotor control. Neuron. 2005;45:953-65.
12. Jurkat-Rott K, Lehmann-Horn F. The impact of splice isoforms on voltage-gated calcium channel alpha1 subunits. J Physiol. 2004;554:609-19.
13. Kanumilli S, Tringham EW, Payne CE, Dupere JR, Venkateswarlu K, Usowicz MM. Alternative splicing generates a smaller assortment of CaV2.1 transcripts in cerebellar Purkinje cells than in the cerebellum. Physiol Genomics. 2006;24:86-96.
14. Kors EE, Haan J, Giffin NJ, Pazdera L, Schnittger C, Lennox GG, Terwindt GM, Vermeulen FL, Van den Maagdenberg AM, Frants RR, Ferrari MD. Expanding the phenotypic spectrum of the CACNA1A gene T666M mutation: a description of 5 families with familial hemiplegic migraine. Arch Neurol. 2003;60:684-8.
15. Krovetz HS, Helton TD, Crews AL, Horne WA. C-Terminal alternative splicing changes the gating properties of a human spinal cord calcium channel alpha 1A subunit. J Neurosci. 2000;20:7564-70.
16. Mintz IM, Venema VJ, Swiderek KM, Lee TD, Bean BP, Adams ME. P-type calcium channels blocked by the spider toxin omega-Aga-IVA. Nature. 1992;355:827-9.
17. Ophoff RA, Terwindt GM, Vergouwe MN, van Eijk R, Oefner PJ, Hoffman SM, Lamerdin JE, Mohrenweiser HW, Bulman DE, Ferrari M, Haan J, Lindhout D, van Ommen GJ, Hofker MH, Ferrari MD, Frants RR. Familial hemiplegic migraine and episodic ataxia type-2 are caused by mutations in the Ca2+ channel gene CACNL1A4. Cell. 1996;87:543-52.
18. Sekirnjak C, Vissel B, Bollinger J, Faulstich M, du Lac S. Purkinje cell synapses target physiologically unique brainstem neurons. J Neurosci. 2003;23:6392-8.
19. Smeyne RJ, Chu T, Lewin A, Bian F, Sanlioglu S, Kunsch C, Lira SA, Oberdick J. Local control of granule cell generation by cerebellar Purkinje cells. Mol Cell Neurosci. 1995;6:230-51.
20. Soong TW, DeMaria CD, Alvania RS, Zweifel LS, Liang MC, Mittman S, Agnew WS, Yue DT. Systematic identification of splice variants in human P/Q-type channel alpha1(2.1)

subunits: implications for current density and Ca2+-dependent inactivation. J Neurosci. 2002;22:10142-52.

21. Tottene A, Fellin T, Pagnutti S, Luvisetto S, Striessnig J, Fletcher C, Pietrobon D. Familial hemiplegic migraine mutations increase Ca(2+) influx through single human CaV2.1 channels and decrease maximal CaV2.1 current density in neurons. Proc Natl Acad Sci U S A. 2002;99:13284-9.
22. van den Maagdenberg AM, Haan J, Terwindt GM, Ferrari MD. Migraine: gene mutations and functional consequences. Curr Opin Neurol. 2007;20:299-305.
23. van den Maagdenberg AMJM, Pizzorusso T, Kaja S, Terpolilli N, Shapovalova N, Hoebeek FE, Barrett CF, Gherardini L, van de Ven RCG, Todorov B, Broos LAM, Tottene A, Gao Z, Fodor M, De Zeeuw CI, Frants RR, Plesnila N, Plomp JJ, Pietrobon D, Ferrari MD. High CSD susceptibility and migraine-associated symptoms in CaV2.1 S218L mice. Ann Neurol. 2010;67:85-98.
24. Walter JT, Alviña K, Womack MD, Chevez C, Khodakhah K. Decreases in the precision of Purkinje cell pacemaking cause cerebellar dysfunction and ataxia. Nat Neurosci. 2006;9:389-97.
25. Westenbroek RE, Sakurai T, Elliott EM, Hell JW, Starr TV, Snutch TP, Catterall WA. Immunochemical identification and subcellular distribution of the alpha 1A subunits of brain calcium channels. J Neurosci. 1995;15:6403-18.